The motion and spin evolution of extended bodies in rotating black hole spacetimes

Zoltán Keresztes[1,†] and Balázs Mikóczi[2,‡]
[1] *Department of Theoretical Physics, University of Szeged, Tisza Lajos krt. 84-86, Szeged 6720, Hungary*
[2] *Research Institute for Particle and Nuclear Physics, Wigner RCP H-1525 Budapest 114, P.O. Box 49, Hungary*
[†] *E-mail: zkeresztes@titan.physx.u-szeged.hu* [‡] *E-mail: mikoczi.balazs@wigner.hu*

We investigate the evolution of spinning bodies moving along zoom-whirl orbits in different rotating (singular/regular) black hole spacetimes. The spinning body approaches the central black hole along the zoom-whirl orbits so much that it enters the ergosphere periodically. The initial data is chosen such that the body would move in the equatorial plane without spin. We illustrate that the spin precessional angular velocity is highly increased near and within the ergosphere when the spin of the body is not nearly parallel to the rotation axis of the central black hole. We discuss the signs of the different black hole spacetimes occurring in the spin precessional dynamics.

I. INTRODUCTION

In general relativity any black hole solution contains a spacetime singularity where the validity of the theory breaks both in the presence and the absence of standard model matter fields. However the inclusion of non-standard matter fields can result in singularity free spacetime solutions describing black holes. In the recent years, the properties of these regular black holes have been widely studied [1–5].

The first metric characterizing the spacetime of a nonrotating regular black hole was proposed by Bardeen [6]. It was interpreted as describing the spacetime surrounding a magnetic monopole which occur in a nonlinear electrodynamic model [7]. The model is defined in terms of an antisymmetric electromagnetic field tensor as the Maxwell theory but the Lagrangian is modified. A nonrotating regular black hole spacetime was also proposed by Hayward [8] which has similar interpretation but with another Lagrangian [9]. A more generic metric containing the subcases suggested by Bardeen and Hayward, and including the rotation of the black hole was derived in Ref. [10].

In this paper we will consider the distinguishability of singular and regular black holes when spinning bodies, practically a much smaller mass black hole compared to the central one, moving about them. We neglect the backreaction of the moving test body to the spacetime curvature, hence use the Mathisson-Papapetrou-Dixon (MPD) equations [11–15] for describing the dynamics. The MPD equations are not closed, a spin supplementary condition (SSC) is necessary to choose [13, 16–23] which defines the point at which the four-momentum and the spin of the body are evaluated.

Analytic computations in case of hyperbolic orbits were carried out for small spin magnitudes whose direction is parallel to the central Kerr black hole rotation axis and when the body moves in the equatorial plane [24]. In this configuration the spin direction is conserved. The spin precession and the orbits when the body approached the centrum from the spatial infinity then it left again into the spatial infinity in both singular and regular black hole spacetimes was studied in Ref. [25]. There the dependencies of the final values of spin and orbital plane orientation angles and azimuthal Boyer-Lindquist coordinate on the initial spin angles and dimensionless specific charge parameter are discussed.

In this paper we focus on zoom-whirl orbits [26–28]. For non-spinning test particles the topology of these orbits was encoded by a rational number [29, 30]. While the zoom-whirl orbits of spinning bodies are more complicated shown within the framework of post-Newtonian dynamics with spin-orbit interaction [31, 32]. Here we will investigate the spin precession along such orbits where the closest approach distance of central black hole is inside the ergosphere. There the post-Newtonian approximation would fail.

The paper is organized as follow. In Section 2 we introduce the MPD equations, the metric characterizing the spacetime of the considered rotating, singular/regular black holes, and two fundamental families of observers, the static and the zero angular momentum ones. We set two frames of comoving observers by boosting the static and the zero angular momentum observers' frames and describe the spin evolution in them. In Section 3 the discussion of the spin precession based on numerical simulations are presented while Section 4 contains the conclusions.

II. THE DYNAMICS OF THE EXTENDED BODIES IN ROTATING, REGULAR BLACK HOLE SPACETIMES

A. Evolution equations

The Mathisson-Papapetrou-Dixon equations [11, 12, 14, 15] read as

$$u^c\nabla_c p^a = -\frac{1}{2}R^a{}_{bcd}u^b S^{cd} \ , \tag{1}$$

$$u^c\nabla_c S^{ab} = p^a u^b - u^a p^b \ . \tag{2}$$

Here ∇_c is the covariant derivative, $R^a{}_{bcd}$ is the Riemann tensor, p^a is the four-momentum of the moving body, S^{ab} is its spin tensor and u^a (with normalization $u^a u_a = -1$) is the four-velocity of the representative point for the extended body determined by the SSC. We use the Tulczyjew-Dixon (TD) SSC [13, 21] imposing that $p_a S^{ab} = 0$. This SSC together with the MPD equations results in two constants of motion: the spin magnitude $S = \sqrt{S_{cd}S^{cd}/2}$ and the dynamical mass $M = \sqrt{-p^a p_a}$. In addition, the TD SSC and the MPD equations yield the following velocity-momentum relation [33]:

$$u^b = \frac{m}{M^2}\left(p^b + \frac{2S^{ba}R_{aecd}p^e S^{cd}}{4M^2 + R_{aecd}S^{ae}S^{cd}}\right) \ , \tag{3}$$

where $m = -u_a p^a$ is the mass measured in the rest frame of the observer moving with velocity u^a.

In addition we introduce a spin four vector as

$$S^a = -\frac{1}{2M}\eta^{abcd}p_b S_{cd} \ , \tag{4}$$

where η_{abcd} is the 4-dimensional Levi-Civita tensor which is totally antisymmetric and $\eta_{0123} = \sqrt{-g}$, where g is the determinant of the metric.

B. Rotating singular and regular black holes

The considered line element squared of rotating black hole spacetimes in Boyer-Lindquist coordinates (t, r, θ, ϕ) [10] [1] is

$$ds^2 = -\frac{\Delta - a^2\sin^2\theta}{\Sigma}dt^2 - \frac{2a\mathcal{B}\sin^2\theta}{\Sigma}dtd\phi + \frac{\Sigma}{\Delta}dr^2 + \Sigma d\theta^2 + \frac{\mathcal{A}}{\Sigma}\sin^2\theta d\phi^2 \ , \tag{5}$$

where a is the rotation parameter, $\Sigma = r^2+a^2\cos^2\theta$, $\Delta = r^2+a^2-2\alpha(r)\,r$, $\mathcal{B} = r^2+a^2-\Delta$, $\mathcal{A} = \left(r^2+a^2\right)^2-\Delta a^2\sin^2\theta$ and[2]

$$\alpha(r) = \mu + \frac{\mu_{em}r^\gamma}{\left(r^\nu + q_m^\nu\right)^{\gamma/\nu}} \ . \tag{6}$$

For a vacuum spacetime $\mu_{em} = 0$, then (5) reduces to the Kerr metric [37] and μ represents the mass parameter of the black hole. The parameter $\mu_{em} = q_m^3/\sigma$ is interpreted as an electromagnetically induced ADM mass by the nonlinear electrodynamic field [38]. The quantity σ in the expression of μ_{em} controls the strength of the nonlinear electrodynamic field and carries the dimension of length squared while q_m is related to the magnetic charge [9]. The spacetime is free from the singularity for $\mu = 0$, $q_m \neq 0$ and $\gamma \geq 3$. In the case of $\mu = 0$ and $\mu_{em} \neq 0$, the powers (γ,ν) are (3,2) for the Bardeen and (3,3) for the Hayward subcases [10].

In our investigation either μ or μ_{em} vanishes. We introduce the notation $\tilde{\mu}$ for the ADM mass which is $\tilde{\mu} = \mu$ for the Kerr spacetime and $\tilde{\mu} = \mu_{em}$ for singularity free spacetimes. The dimensionless line element squared $ds^2/\tilde{\mu}^2$ can be expressed in terms of $t/\tilde{\mu}$, $r/\tilde{\mu}$, θ, ϕ and $a/\tilde{\mu}$ with $\alpha/\mu = 1$ in case of Kerr spacetime and $\alpha(r)/\mu_{em} = (r/\mu_{em})^\gamma / \left[(r/\mu_{em})^\nu + q^\nu\right]^{\gamma/\nu}$ with $q = q_m/\mu_{em}$ in cases of singularity free spacetimes. The latter shows that the structure of singularity free spacetimes is determined by the dimensionless specific charge parameter[3] q, the dimensionless rotation parameter a/μ_{em} and the ADM mass μ_{em} (which gives a distance scale). In the limit $q \to 0$ with $\mu_{em} \neq 0$ (hence both $\sigma \to 0$ and $q_m \to 0$) we obtain $\alpha(r)/\mu_{em} = 1$ which corresponds to the Kerr spacetime with mass parameter $\mu = \mu_{em}$ [10].

The stationary limit surfaces and the event horizons (if they exist) are determined by the solutions of $g_{tt} = 0$ and $g^{rr} = 0$, respectively. The region which is located outside the outer event horizon but inside the outer stationary limit surface is called ergosphere. The existence of the stationary limit surfaces and the event horizons are strongly dependent on the parameters a/μ_{em} and q, see Figs. 3 and 4 in Ref. [10]. For the chosen parameter values in the next section, the regular black holes will have similar structure as the Kerr spacetime, i.e. they have two event horizons and two stationary limit surfaces.

C. Spin precession angular velocities in different comoving frames

We describe the spin dynamics in both comoving frames which are obtained by boost transformations from either the frame of static observers or that of the zero angular momentum observers. The frame of static observers (SOs) is given by

$$e_{\mathbf{0}} = u_{(SO)} = \frac{1}{\sqrt{-g_{tt}}}\partial_r \ , \ e_{\mathbf{1}} = \sqrt{\frac{\Delta}{\Sigma}}\partial_r \ , \ e_{\mathbf{2}} = \frac{\partial_\theta}{\sqrt{\Sigma}} \ , \ e_{\mathbf{3}} = -\frac{1}{\sqrt{\Delta}}\left(\frac{a\mathcal{B}\sin\theta}{\Sigma\sqrt{-g_{tt}}}\partial_t - \frac{\sqrt{-g_{tt}}}{\sin\theta}\partial_\phi\right) \ , \tag{7}$$

---

[1] There are discussions [34–36] on that the rotating regular black hole spacetimes derived in Ref. [10] are not exact solutions of the field equations. However the analytically presented spacetime family may differ perturbatively from the exact solution [36], therefore it is suitable for consideration of the evolution of spinning bodies.

[2] Correspondence between notations used throughout this article and Ref. [10]: $\mu \to M$, $\mu_{em} \to M_{em}$, $q_m \to q$, $\alpha(r) \to \rho(r)$.

[3] The notation is the same for this parameter in Ref. [10].

while that of the zero angular momentum observers (ZAMOs) by

$$f_{\mathbf{0}} = u_{(ZAMO)} = \sqrt{\frac{\mathcal{A}}{\Sigma\Delta}}\left(\partial_t + \frac{a\mathcal{B}}{\mathcal{A}}\partial_\phi\right) \ , \ f_{\mathbf{1}} = \sqrt{\frac{\Delta}{\Sigma}}\partial_r \ , \ f_{\mathbf{2}} = \frac{\partial_\theta}{\sqrt{\Sigma}} \ , \ f_{\mathbf{3}} = \sqrt{\frac{\Sigma}{\mathcal{A}}}\frac{\partial_\phi}{\sin\theta} \ . \tag{8}$$

The boosted comoving frames are obtained [39] as

$$E_{\mathbf{0}}\left(e,u\right) = u \ , \ E_\alpha\left(e,u\right) = e_\alpha + \frac{u\cdot e_\alpha}{1+\Gamma_{(S)}}\left(u + u_{(SO)}\right) \ , \tag{9}$$

and

$$E_{\mathbf{0}}\left(f,u\right) = u \ , \ E_\alpha\left(f,u\right) = f_\alpha + \frac{u\cdot f_\alpha}{1+\Gamma_{(Z)}}\left(u + u_{(ZAMO)}\right) \ , \tag{10}$$

with frame indices $\alpha = \{\mathbf{1},\mathbf{2},\mathbf{3}\}$ and Lorentz factors $\Gamma_{(S)} = -u\cdot u_{(SO)}$ and $\Gamma_{(Z)} = -u\cdot u_{(ZAMO)}$. The dot denotes the inner product with respect to the background spacetime metric. A spatial rotation about the axis n^α with nonvanishing components

$$n^{\mathbf{1}} = -\frac{w^{\mathbf{2}}_{(Z)}}{\sqrt{\left(w^{\mathbf{1}}_{(Z)}\right)^2 + \left(w^{\mathbf{2}}_{(Z)}\right)^2}} \text{ and } \ n^{\mathbf{2}} = \frac{w^{\mathbf{1}}_{(S)}}{\sqrt{\left(w^{\mathbf{1}}_{(S)}\right)^2 + \left(w^{\mathbf{2}}_{(S)}\right)^2}} \tag{11}$$

by an angle Θ determined from

$$\sin\Theta = -\left[\left(1 - \sqrt{\frac{\Sigma\Delta}{-g_{tt}\mathcal{A}}}\right)\frac{\Gamma_{(S)}w^{\mathbf{3}}_{(S)}}{1+\Gamma_{(S)}} - \frac{a\mathcal{B}\sin\theta}{\sqrt{-g_{tt}\Sigma\mathcal{A}}}\right]\frac{\Gamma_{(S)}\sqrt{\left(w^{\mathbf{1}}_{(S)}\right)^2 + \left(w^{\mathbf{2}}_{(S)}\right)^2}}{1+\Gamma_{(Z)}} \ , \tag{12}$$

transforms the frame vectors $E_{\mathbf{A}}\left(e,u\right)$ to $E_{\mathbf{A}}\left(f,u\right)$ (where $\mathbf{A} = \{\mathbf{0},\mathbf{1},\mathbf{2},\mathbf{3}\}$). Here $\mathbf{w}_{(S)} = \Gamma^{-1}_{(S)}u_{(SO)} - u$ and $\mathbf{w}_{(Z)} = \Gamma^{-1}_{(Z)}u_{(ZAMO)} - u$ are the relative spatial velocities of the SO and ZAMO, respectively, with respect to the moving body in the comoving frame.

Following Refs. [39] and [25], we introduce Cartesian-like 3-bases $(e_{\mathbf{x}}, e_{\mathbf{y}}, e_{\mathbf{z}})$ and $(f_{\mathbf{x}}, f_{\mathbf{y}}, f_{\mathbf{z}})$ in the local rest spaces of SOs and ZAMOs, respectively, by the definitions $(e_{\mathbf{1}}, e_{\mathbf{2}}, e_{\mathbf{3}}) = (e_{\mathbf{x}}, e_{\mathbf{y}}, e_{\mathbf{z}})\,R\left(\theta,\phi\right)$ and $(f_{\mathbf{1}}, f_{\mathbf{2}}, f_{\mathbf{3}}) = (f_{\mathbf{x}}, f_{\mathbf{y}}, f_{\mathbf{z}})\,R\left(\theta,\phi\right)$. Here $R\left(\theta,\phi\right)$ is the same rotation matrix

$$R\left(\theta,\phi\right) = \begin{pmatrix} \sin\theta\cos\phi & \cos\theta\cos\phi & -\sin\phi \\ \sin\theta\sin\phi & \cos\theta\sin\phi & \cos\phi \\ \cos\theta & -\sin\theta & 0 \end{pmatrix} \ , \tag{13}$$

which locally relates the unit basis vectors of Cartesian and spherical coordinates in the 3-dimensional Euclidean space. The orbit of the spinning body will be represented by the corresponding Cartesian-like coordinates $x = r\cos\phi\sin\theta$, $y = r\sin\phi\sin\theta$ and $z = r\cos\theta$.

The evolution equations for the Cartesian-like frame components of the spin vector derived from the MPD equations are given by

$$\frac{dS^{\mathbf{i}}}{d\tau} = -R^{\mathbf{i}}{}_\alpha\varepsilon^\alpha{}_{\beta\gamma}\Omega^\beta_{(prec)}S^\gamma \ , \tag{14}$$

where $\mathbf{i} = \{\mathbf{x},\mathbf{y},\mathbf{z}\}$, $\alpha,\ \beta,\ \gamma = \{\mathbf{1},\mathbf{2},\mathbf{3}\}$, $\varepsilon_{\alpha\beta}{}^\gamma$ is the 3-dimensional Levi-Civita symbol and $R^{\mathbf{i}}{}_\alpha$ stands for the components of rotation matrix. Hence the dynamics is encoded in the precessional angle velocity

$$\Omega^\beta_{(prec)} = -\Omega^\beta_{(orb)} + \Omega^\beta \ , \tag{15}$$

where $\Omega^{\mathbf{1}}_{(orb)} = \cos\theta\dot{\phi}$, $\Omega^{\mathbf{2}}_{(orb)} = -\sin\theta\dot{\phi}$, $\Omega^{\mathbf{3}}_{(orb)} = \dot{\theta}$ and $\Omega^{\mathbf{1}} = E_{\mathbf{3}}\cdot DE_{\mathbf{2}}/d\tau$, $\Omega^{\mathbf{2}} = -E_{\mathbf{3}}\cdot DE_{\mathbf{1}}/d\tau$, $\Omega^{\mathbf{3}} = E_{\mathbf{2}}\cdot DE_{\mathbf{1}}/d\tau$. However the parallel component of $\Omega^\beta_{(prec)}$ with s^γ does not influence on the spin precession due to the cross product on the right hand side of Eq. (14), only its perpendicular component

$$\tilde{\Omega}^\beta_{(prec)} = \Omega^\beta_{(prec)} - \frac{\delta_{\alpha\gamma}\Omega^\alpha_{(prec)}S^\gamma}{S^2}S^\beta \tag{16}$$

which is count.

When describing the evolution in the Cartesian boosted SO (ZAMO) frame we use $E_\alpha\left(e,u\right)$ $(E_\alpha\left(f,u\right))$ vectors in the expression of Ω^β hence obtaining $\Omega^\beta(e,u)$ $(\Omega^\beta(f,u))$, $\Omega^\beta_{(prec)}(e,u)$ $(\Omega^\beta_{(prec)}(f,u))$ and $\tilde{\Omega}^\beta_{(prec)}(e,u)$ $(\tilde{\Omega}^\beta_{(prec)}(f,u))$.

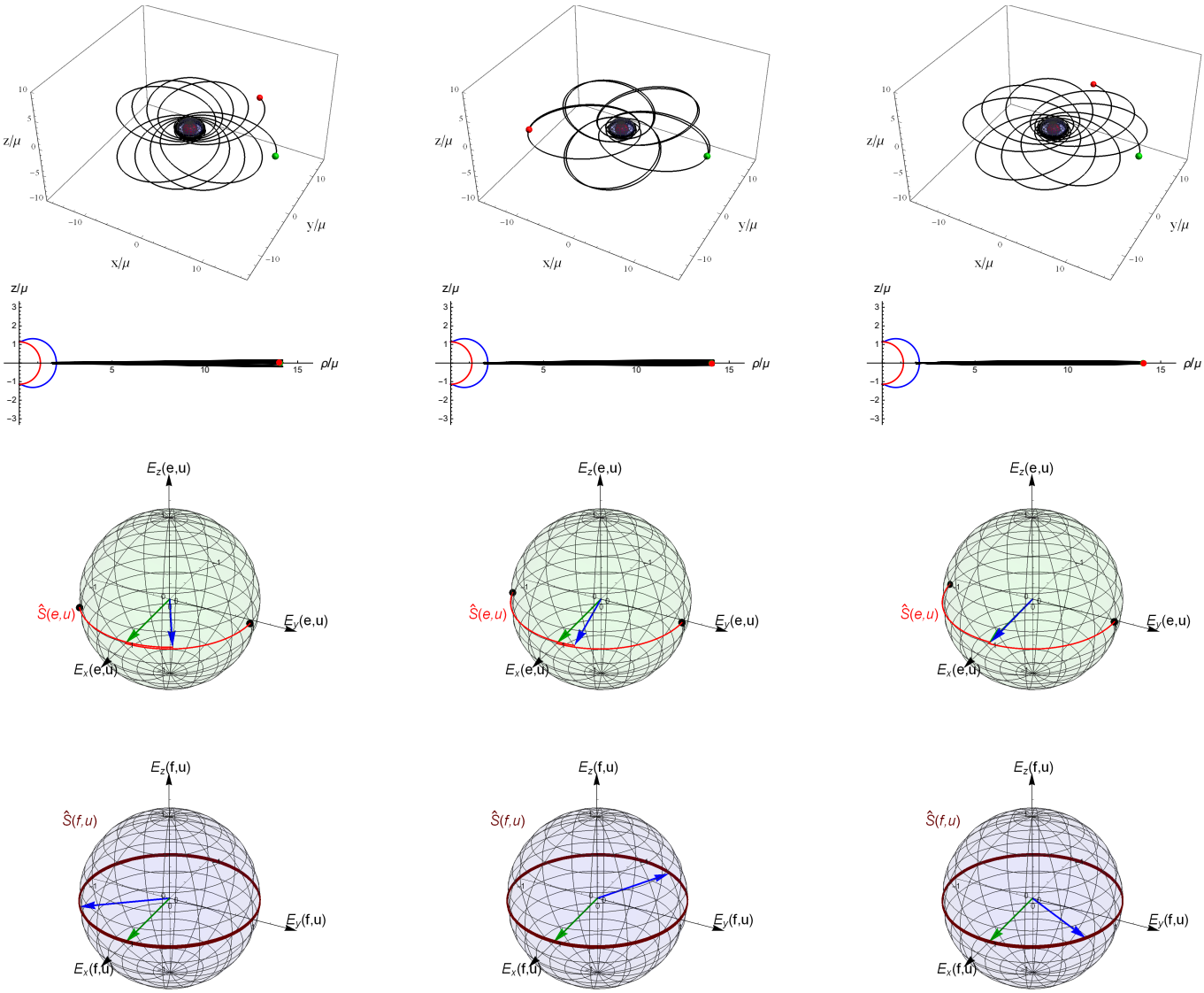

FIG. 1. The evolutions along zoom-whirl orbits with initial spin polar angle $\theta^{(S)}(0) = \pi/2$ and rotation parameter rotation parameter $a = 0.99\tilde{\mu}$. The first column represents the evolution for the two cases: when the background spacetime is either the Kerr or the rotating Hayward with $q = 0.081$ (they are only perturbatively differ from each other). In case of the middle and the right columns the central black hole are the rotating Hayward with $q = 0.216$ and the rotating Bardeen with $q = 0.081$. The rows represent the following: 1st and 2nd the orbit in the coordinate spaces (x,y,z) and (ρ,z), 3th and 4th the unit spin vector in the boosted SO and ZAMO comoving Cartesian-like frames, respectively.

III. NUMERICAL INVESTIGATION

We consider the evolution of spinning bodies which follow zoom-whirl orbits crossing through the ergosphere of singular and regular black holes. The body starts at $\theta(0) = \pi/2$, $r(0) = 14.05\tilde{\mu}$ and $\phi(0) = 0 = t(0)$ while the independent components of the initial four momentum are $p^r(0)/M = -0.03$, $\tilde{\mu}p^{\phi}(0)/M = 0.012$ and $\tilde{\mu}p^{\theta}(0)/M = 0$. The initial spin vector of the body is characterized in the comoving Cartesian frame set up by boosting the SO frame. Thus

$$S = S^{\mathbf{i}} E_{\mathbf{i}}(e,u) \ , \tag{17}$$

where $\mathbf{i} = \{\mathbf{x},\mathbf{y},\mathbf{z}\}$ and

$$S^{\mathbf{i}} = |S| \left(\cos\phi^{(S)} \sin\theta^{(S)}, \sin\phi^{(S)} \sin\theta^{(S)}, \cos\theta^{(S)}\right) \ . \tag{18}$$

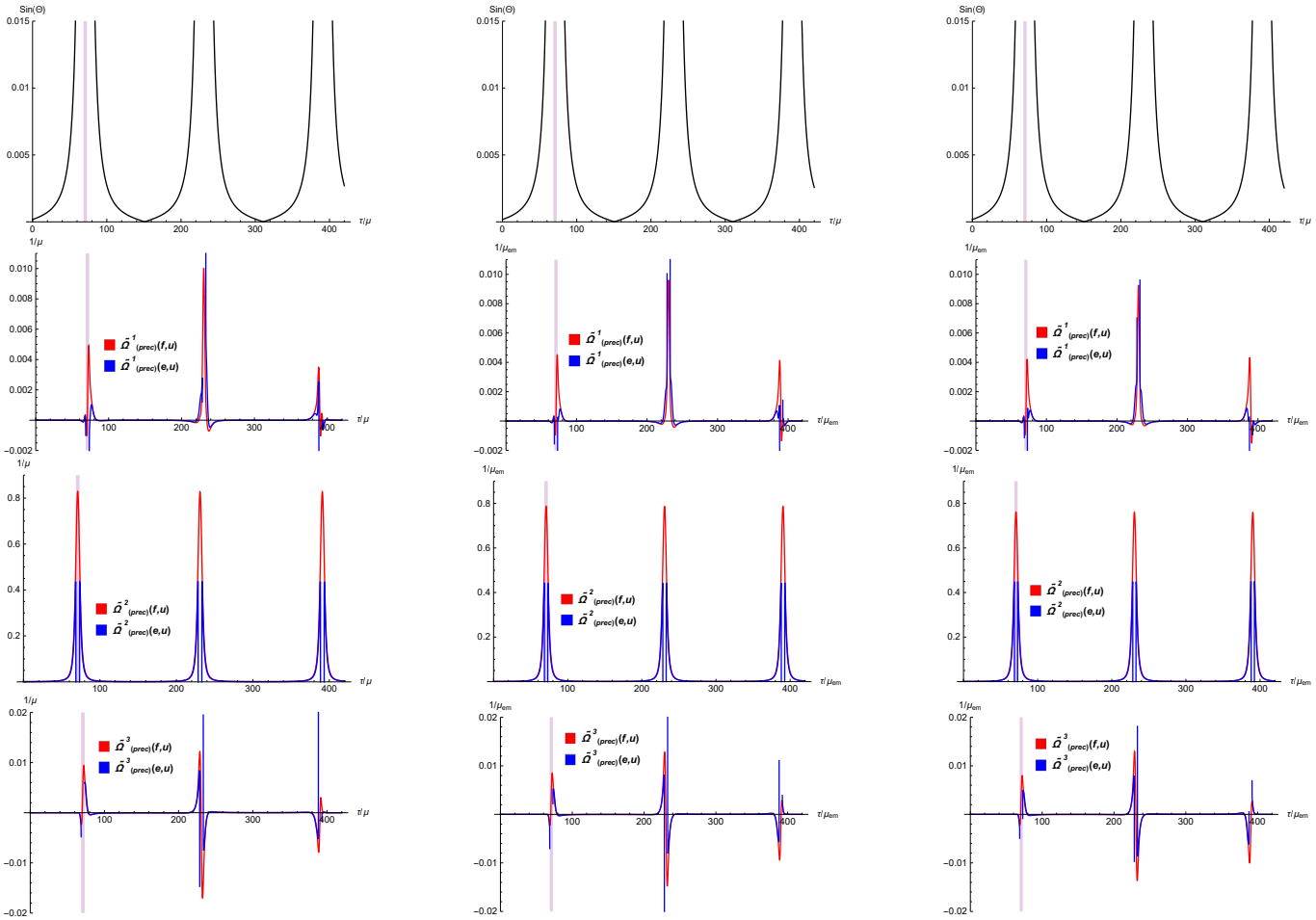

FIG. 2. The evolution of $\sin\Theta$ and the spherical comoving triad components of the spin precessional velocities $\tilde{\Omega}^{\alpha}_{(prec)}(e,u)$ and $\tilde{\Omega}^{\alpha}_{(prec)}(f,u)$ in the boosted SO (blue lines) and ZAMO (red lines) frames, respectively, along the same orbits (but containing only the first three zoom period) presented in the columns of Fig. 1.

TABLE I. The coefficients c_i of quadratic polynomial function shown on Fig. 4.

BHs	c_2	c_1	c_0
Kerr	-0.4020	1.2784	-0.0237
Hayward, $q=0.081$	-0.4002	1.2725	-0.0240
Hayward, $q=0.216$	-0.3707	1.1772	-0.0290
Bardeen, $q=0.081$	-0.3608	1.1229	0.0188

The angles $\theta^{(S)}$ and $\phi^{(S)}$ are the spherical polar angles of the spin vector in the comoving Cartesian frame. The spin magnitude and the initial spin azimuthal angle will be chosen as $|S|/\tilde{\mu}M=0.01$ and $\phi^{(S)}(0)=0$.

We choose $\gamma=3$. The background will be either a regular, rotating Bardeen ($\nu=2$) or Hayward ($\nu=3$) black hole spacetime. There is always a black hole in the singularity free spacetimes in the range $a\leq 0.99\mu_{em}$ if $q\leq 0.081$ for $\nu=2$ and $q\leq 0.216$ for $\nu=3$, respectively. The event horizon disappears for the higher values of q if $a=0.99\mu_{em}$.

The first row of Fig. 1 shows typical zoom-whirl orbits in the (x,y,z)-space with initial spin polar angle $\theta^{(S)}(0)=\pi/2$ and rotation parameter $a=0.99\tilde{\mu}$. The first column represents the evolution for the two cases: when the background spacetime is either the Kerr or the rotating Hayward with $q=0.081$. The evolutions only differ pertubatively from each other in these cases. The background spacetimes in the second and the third columns are the rotating Hayward with $q=0.216$ and the rotating Bardeen with $q=0.081$, respectively. The initial and the final positions of the

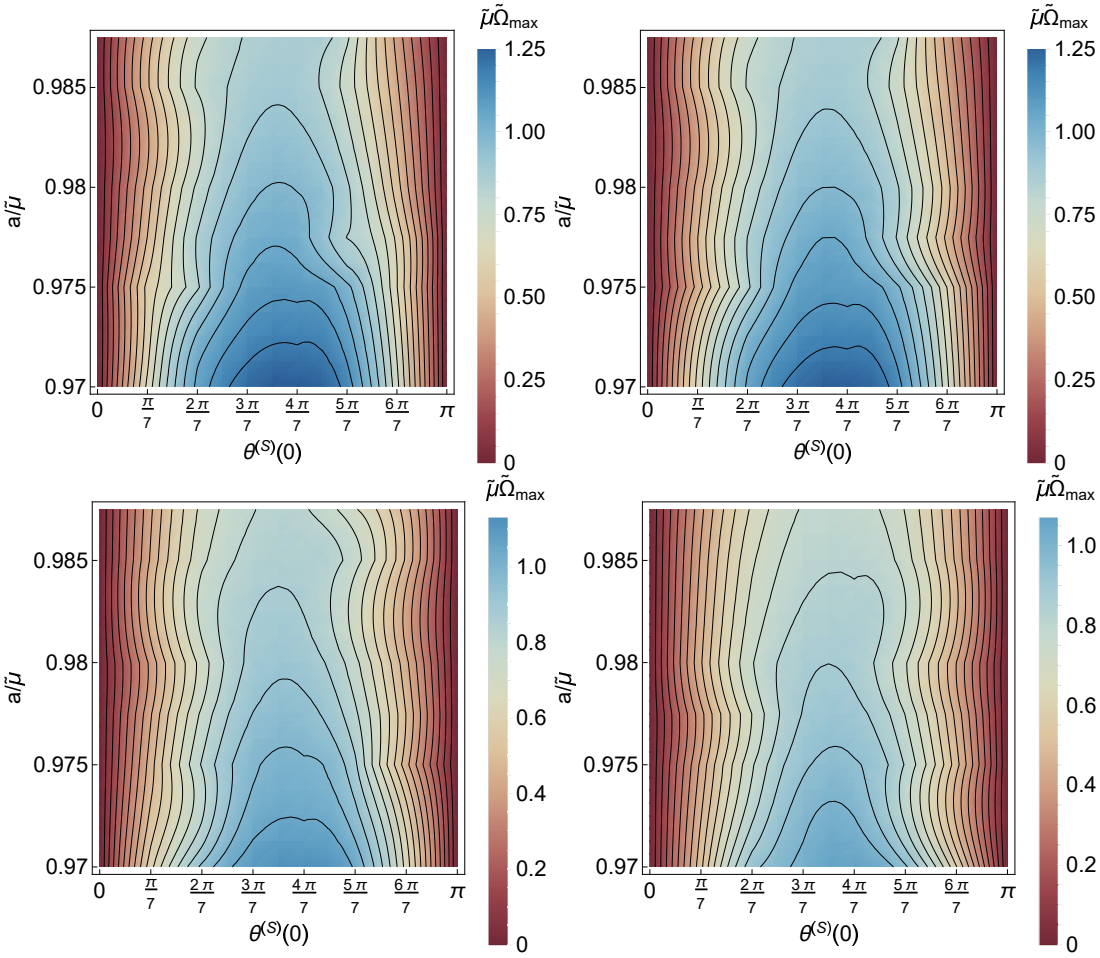

FIG. 3. The maximum of the magnitude ($\tilde{\Omega}_{\max}$) of $\tilde{\Omega}^{\alpha}_{(prec)}(f,u)$ during the first zoom period is shown in the parameter plane $(\theta^{(s)}(0), a/\tilde{\mu})$. From top left to bottom right the background spacetimes are the Kerr, the rotating Hayward with $q = 0.081$, the rotating Hayward with $q = 0.216$ and the rotating Bardeen with $q = 0.081$.

body are marked by green and red dots. The blue surface at the centre depicts the outer bound of the black hole's ergosphere. The second row shows the same orbits in the $(\rho = r\sin\theta, z = r\cos\theta)$ coordinate space. The third and fourth rows image the evolutions of the unit spin vector represented in the boosted SO and ZAMO Cartesian frames, respectively. Since SOs exist only outside of the ergosphere, the spin evolution cannot be represented in the boosted SO frame when the body stays in that region. The jump in the evolution of the spin vector in the boosted SO frame (marked by black dots) emphasizes that a relatively large part of the variation in the spin direction takes place inside the ergosphere.

The first row of Fig. 2 show the evolutions of the rotation angle Θ defined by Eq. (12). The columns represent the same cases as that of Fig. 1 but only presenting that part of the evolutions which contains the first three zoom period where the body approaches the central black hole. The purplish shadow represent the first period when the body is inside the ergosphere. The angle Θ is small when the body is relatively far from the central black hole, hence the boosted SO and ZAMO frames differ only slightly there. The additional three rows image the spherical comoving triad components of precessional angular velocities $\tilde{\Omega}^{\alpha}_{(prec)}(e,u)$ and $\tilde{\Omega}^{\alpha}_{(prec)}(f,u)$ both in the boosted SO (blue line) and ZAMO (red line) frames. The blue lines diverge at the location of the outer stationary surface because SOs exist only outside of the ergosphere. However the boosted ZAMO frame can be used for description of the spin precession inside the ergosphere. The red curves show that the spin precessional velocities are highly increased near the centrum.

The maximum of the magnitude $\tilde{\Omega}_{\max}$ of $\tilde{\Omega}^{\alpha}_{(prec)}(f,u)$ during the first zoom period is shown in the parameter plane $(\theta^{(s)}(0), a/\tilde{\mu})$ on Fig. 3. We note that zoom-whirl orbits do not develop for $a/\tilde{\mu} < 0.97$ with the used initial values because the body crosses the event horizon. In the upper row, the two panel representing the cases when the background either the Kerr (left) or the rotating Hayward with $q = 0.081$ (right) show considerable differences

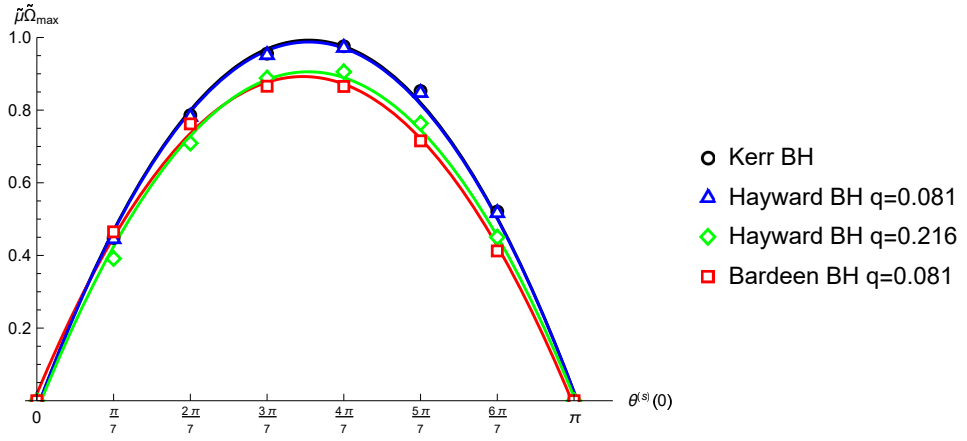

FIG. 4. The dependence of $\tilde{\mu}\tilde{\Omega}_{\rm max}$ on $\theta^{(s)}(0)$ for $a/\widetilde{\mu} = 0.98$ is shown when the spinning body moves about singular/regular black holes. The coefficients of the fitted quadratic polynomial function $c_2X^2 + c_1X + c_0$ with $X = \tilde{\mu}\tilde{\Omega}_{\rm max}$ is given in Table I for each cases.

in the right middle region. The dimensionless specific charge parameter in the second row takes those largest value ($q = 0.216$ for the rotating Hayward and $q = 0.081$ for the rotating Bardeen case) where the event horizon surrounding the centrum does not disappear in the range $a \leq 0.99\mu_{em}$. These maps are significantly differ from the Kerr case along a wide stripe around $\theta^{(s)}(0) = \pi/2$. The rotating Hayward (left) and the rotating Bardeen (right) cases are also well distinguishable along this stripe.

For a fixed rotation parameter the dependence of $\tilde{\Omega}_{\rm max}$ on $\theta^{(s)}(0)$ can be described roughly by a quadratic function which is shown on Fig. 4 with $a = 0.98\tilde{\mu}$. The coefficients c_i of the fitted quadratic function is presented in Table I. We see that there is no considerable difference between the Kerr and the rotating Hayward with $q = 0.081$ subcases. While the other two cases significantly differ from these and from each other around $\theta^{(s)}(0) = \pi/2$. However this stands for the case $a = 0.98\tilde{\mu}$. On Fig. 5 we present how depend the coefficients c_i ($i = 0,\ 1,\ 2$) of the quadratic function on the rotation parameter in case of singular and regular black hole spacetimes. These functions supports that the singular and regular (for sufficiently large values of q) black hole spacetimes can be distinguished by considering the spin precession of a such moving body which significantly approaches the centre.

IV. CONCLUSION

We have studied the evolution of spinning bodies moving on zoom-whirl orbits. At the closest approach distance of the central rotating, singular/regular black hole, the body crossed the ergosphere. In the considered numerical simulations the initial values were chosen such that the relatively small mass body without spin would have moved in the equatorial plane. However since the initial spin was not aligned or anti-aligned with the rotation axis of the central black hole, the body moved out of the equatorial plane. Apart from narrow stripes at $\theta^{(S)}(0) = 0$ and π, the spin precession was highly increased close to and within the ergosphere. The maximum of the dimensionless spin precessional angular velocity $\tilde{\mu}\tilde{\Omega}_{\rm max}$ depended significantly on the black hole rotation parameter a, the dimensionless specific charge parameter q and the initial polar spin angle $\theta^{(s)}(0)$. The limit $q \to 0$ with $\mu_{em} \neq 0$ of the rotating Hayward and Bardeen spacetimes result in the Kerr black hole. Otherwise ($q \neq 0$) the rotating Hayward and the Bardeen spacetimes are free from the singularity. For a fixed a and q, the dependence of $\tilde{\mu}\tilde{\Omega}_{\rm max}$ on $\theta^{(s)}(0)$ is roughly described by a quadratic function. For sufficiently large values of q, $\tilde{\mu}\tilde{\Omega}_{\rm max}$ has showed significantly different dependence on both a and $\theta^{(s)}(0)$ in cases of the central singular and regular black holes.

V. ACKNOWLEDGEMENTS

The work of Z. K. was supported by the János Bolyai Research Scholarship of the Hungarian Academy of Sciences, by the UNKP-20-5 New National Excellence Program of the Ministry of Human Capacities and by the Hungarian National Research Development and Innovation Office (NKFI) in the form of the grant 123996. The work of B. M.

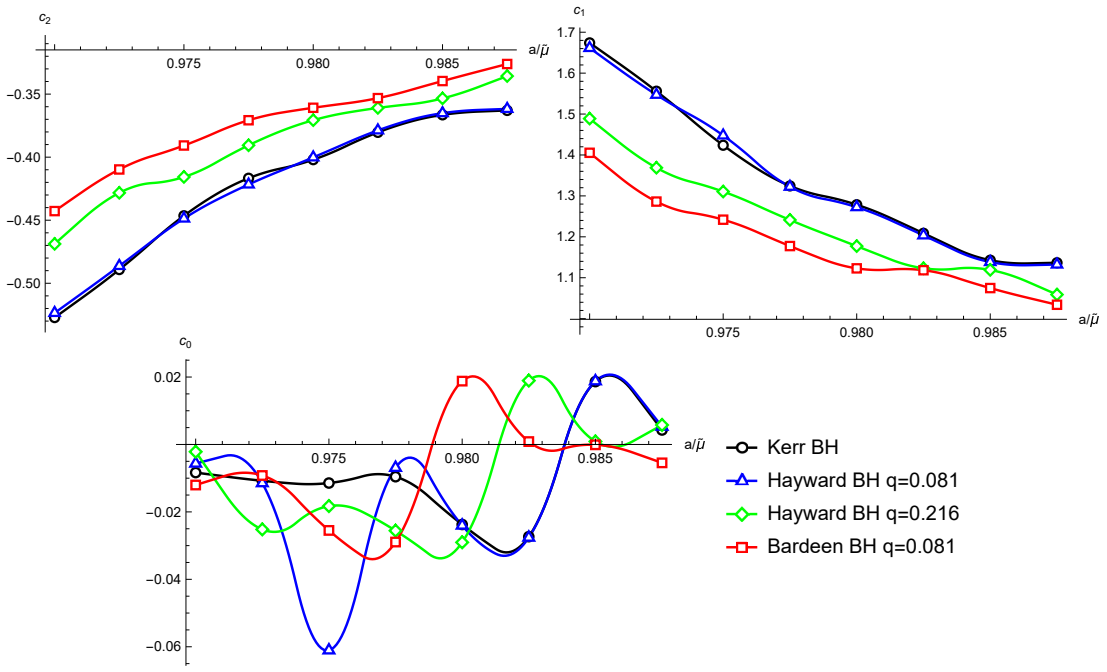

FIG. 5. The dependence of coefficients c_i on $a/\widetilde{\mu}$ in the cases of singular and regular background black hole spacetimes.

was supported by the János Bolyai Research Scholarship of the Hungarian Academy of Sciences.

[1] Bianchi, E., De Lorenzo, T., and Smerlak, M.: 2015, Entanglement entropy production in gravitational collapse: covariant regularization and solvable models. *JHEP* **06**, 180.
[2] Toshmatov, B., Abdujabbarov, A., Stuchlík, Z., and Ahmedov, B.: 2015, Quasinormal modes of test fields around regular black holes. *Phys. Rev. D* **91**, 083008.
[3] Abdujabbarov, A., Amir, M., Ahmedov, B., and Ghosh, S.G.: 2016, Shadow of rotating regular black holes. *Phys. Rev. D* **93**, 104004.
[4] Maluf, R.V., and Neves, J.C.S.: 2018, Thermodynamics of a class of regular black holes with a generalized uncertainty principle. *Phys. Rev. D* **97**, 104015.
[5] Toshmatov, B., Stuchlík, Z., Ahmedov, B. and Malafarina, D.: 2019, Relaxations of perturbations of spacetimes in general relativity coupled to nonlinear electrodynamics. *Phys. Rev. D* **99**, 064043.
[6] Bardeen, J.M.: 1968, Non-singular general-relativistic gravitational collapse. *Proc. GR5, Tbilisi USSR*, 174.
[7] Ayán-Beato, E., and García, A.: 2000, The Bardeen Model as a Nonlinear Magnetic Monopole. *Phys. Lett. B* **493**, 149.
[8] Hayward, S.A.: 2006, Formation and evaporation of non-singular black holes. *Phys. Rev. Lett.* **96**, 031103.
[9] Fan, Z.-Y., and Wang, X.: 2016, Construction of Regular Black Holes in General Relativity. *Phys. Rev. D* **94**, 124027.
[10] Toshmatov, B., Stuchlík, Z., and Ahmedov, B.: 2017, Generic rotating black holes in general relativity coupled to nonlinear electrodynamics. *Phys. Rev. D* **95**, 084037.
[11] Mathisson, M.: 1937, Neue Mechanik Materieller Systeme. *Acta. Phys. Polon.* **6**, 163.
[12] Papapetrou, A.: 1951, Equations of Motion in General Relativity. *Proc. Phys. Soc.* **64**, 57.
[13] Dixon, W.G.: 1964, A covariant multipole formalism for extended test bodies in general relativity. *Nuovo Cim.* **34**, 317.
[14] Dixon, W.G.: 1970, Dynamics of Extended Bodies in General Relativity. I. Momentum and Angular Momentum. *Proc. R. Soc. London A* **314**, 499.
[15] Dixon, W.G.: 1979, Extended Bodies in General Relativity: Their Description and Motion.*Proceedings of the International School of Physics, Course LXVII, ed. by J. Ehlers.*
[16] Frenkel, J.: 1926, Die Elektrodynamik des rotierenden Elektrons. *Z. Phys.* **37**, 243.
[17] Pirani, F.A.E.: 1926, On the Physical significance of the Riemann tensor. *Acta Phys. Polon.* **15**, 389.
[18] Corinaldesi, E., and Papapetrou, A.: 1951, Spinning Test-Particles in General Relativity II. *Proc. Roy. Soc. A* **209**, 259.
[19] Newton, T.D., and Wigner, E.P.: 1949, Localized States for Elementary Systems. *Rev. Mod. Phys.* **21**, 400.
[20] Pryce, M.H.L.: 1948, The Mass-Centre in the Restricted Theory of Relativity and Its Connexion with the Quantum Theory of Elementary Particles, *Proc. Roy. Soc. Lond. A* **195**, 62.

[21] Tulczyjew, W.M.: 1959, Motion of multipole particles in general relativity theory. *Acta Phys. Polon.* **18**, 393.

[22] Ohashi, A.: 2003, Multipole particle in relativity. *Phys. Rev. D* **68**, 044009.

[23] Kyrian, K., and Semerák, O.: 2007, Spinning test particles in a Kerr field - II. *Mon. Not. Roy. Astron. Soc.* **382**, 1922.

[24] Bini, D., Geralico, A., and Vines, J.: 2017, Hyperbolic scattering of spinning particles by a Kerr black hole. *Phys. Rev. D* **96**, 084044.

[25] Keresztes, Z., and Mikóczi, B.: 2020, The motion and spin evolution of extended bodies in rotating black hole spacetimes. *Romanian Astron. J.* , Vol. **30**, No. 1, p. 61.

[26] Glampedakis, K., and Kennefick, D.: 2002, Zoom and whirl: Eccentric equatorial orbits around spinning black holes and their evolution under gravitational radiation reaction. *Phys. Rev. D* **66**, 044002.

[27] Glampedakis, K., Hughes, S.A., and Kennefick, D.: 2002, Approximating the inspiral of test bodies into Kerr black holes. *Phys. Rev. D* **66**, 064005.

[28] Glampedakis, K.: 2005, Extreme Mass Ratio Inspirals: LISA's unique probe of black hole gravity. *Class. Quant. Grav.* **22**, S605.

[29] Levin, J., and Perez-Giz, G.: 2008, A periodic table for black hole orbits. *Phys. Rev. D* **77**, 103005.

[30] Grossman, R., Levin, J., and Perez-Giz, G.: 2012, The harmonic structure of generic Kerr orbits. *Phys. Rev. D* **85**, 023012.

[31] Levin, J., and Grossman, R.: 2009, Dynamics of black hole pairs. I. Periodic tables. *Phys. Rev. D* **79**, 043016.

[32] Grossman, R., and Levin, R.: 2009, Dynamics of black hole pairs. II. Spherical orbits and the homoclinic limit of zoom-whirliness. *Phys. Rev. D* **79**, 043017.

[33] Semerák, O.: 1999, Spinning test particles in a Kerr field - I. *Mon. Not. Roy. Astron. Soc.* **308**, 863.

[34] Bronnikov, K.A.: 2017, Comment on "Construction of regular black holes in general relativity". *Phys. Rev. D* **96**, 128501.

[35] Rodrigues, M.E., and Junior, E.L.B.: 2017, Comment on "Generic rotating regular black holes in general relativity coupled to non-linear electrodynamics". *Phys. Rev. D* **96**, 128502.

[36] Toshmatov, B., Stuchlík, Z., and Ahmedov, B.: 2017, Note on the character of the generic rotating charged regular black holes in general relativity coupled to nonlinear electrodynamics. [arXiv:1712.04763].

[37] Kerr, R.P.: 1963, Gravitational Field of a Spinning Mass as an Example of Algebraically Special Metrics. *Phys. Rev. Lett.* **11**, 237

[38] Toshmatov, B., Stuchlík, Z., and Ahmedov, B.: 2018, Comment on "Construction of regular black holes in general relativity. *Phys. Rev. D* **98**, 028501.

[39] Bini, D., Geralico, A., and Jantzen, R.T.: 2017, Gyroscope precession along general timelike geodesics in a Kerr black hole spacetime. *Phys. Rev. D* **95**, 124022.